THE ASTROPHYSICAL JOURNAL, 251:451–464, 1981 December 15


# Fe II EMISSION IN QUASARS

STEVEN A. GRANDI
Department of Astronomy, University of California, Los Angeles
*Received 1981 March 2; accepted 1981 June 18*

## ABSTRACT

In an attempt to understand Fe II emission in quasars, observations of Fe II blends at λ2100, λ2500, λ2950, λ3200, λ4570, λλ5190,5320 as well as Mg II λ2798, the Balmer lines and continuum, and the power law spectral index are reported for 38 quasars and high redshift Seyfert 1 galaxies. Considering only relative strengths among the UV Fe II blends, which should be insensitive to column density effects, the observed blend strengths agree well with predicted strengths from optically thick collisional excitation models for Fe II emission. However, synthetic spectra based on two extensive Fe II calculations (due to Phillips and to Kwan and Krolik) disagree rather badly with observed quasar spectra. Based on an ad hoc exercise in modifying the predicted multiplet strengths to force a better fit, it is concluded that future correct models of Fe II emission in quasars should include many more terms (low lying doublet terms and terms near 8 eV) than have been included previously, and that electron temperatures higher than 10,000 K should be considered.

*Subject headings:* line identifications — quasars — spectrophotometry

## I. INTRODUCTION

Blends of the numerous emission lines of Fe II have been a recognized part of the optical spectra of Seyfert 1 galaxies and quasars since the work of Wampler and Oke (1967) and Baldwin (1975*a*) and have been extensively discussed by Phillips (1978*a*). Recently, despite earlier claims to the contrary, UV Fe II blends have been recognized as quite common, if not ubiquitous, in the spectra of quasars and high redshift Seyfert 1 galaxies (Wills *et al.* 1980; Wills, Netzer, and Wills 1980; Grandi and Phillips 1980). In fact, many features previously identified in quasar spectra such as C II] λ2326, He II λ3203, He I λ3188, and numerous forbidden lines are almost certainly Fe II blends instead.

Two mechanisms have been proposed to excite the optical Fe II emission. These optical multiplets arise from transitions from odd parity terms near 5 eV to even parity terms near 3 eV above the ground state. In one mechanism, the 5 eV terms are radiatively pumped by absorption of continuum photons in resonance lines from the lowest few terms of Fe II. In the second mechanism, the 5 eV terms are pumped by collisions with electrons. In both cases, the optical multiplets, which generally have low branching rations, will be observed if the optical depth in the colevel resonance lines is sufficiently high.

Until recently, the continuum resonance fluorescence mechanism enjoyed favor (see Phillips 1978*b*), buoyed by reasonable agreement between predictions and observations and by the fact that the optical Fe II emission seems to be much too strong compared to the collisionally excited Mg II λ2798 line to be also due to collisional excitation. However, the discovery that many of the "bumps and wiggles" seen in the UV spectra of quasars (redshifted into the observed visible) could consistently and coherently be identified as Fe II emission blends, including the resonance lines to the 5 eV terms, has cast great doubt on the continuum resonance fluorescence model, since in that model the 5 eV resonance lines should almost certainly be seen in absorption. Also, recent theoretical investigations (Netzer 1980; Collin-Souffrin *et al.* 1979, 1980) have shown that there are insufficient continuum photons to excite the observed optical lines by fluorescence; these investigations have also shown that the Mg II λ2798 strength will be limited by various effects in real quasar emission line regions, thus invalidating the comparison of collisionally excited optical Fe II emission to Mg II λ2798. Therefore, the optically thick collisional excitation model seems to be the best explanation for both the observed optical and UV Fe II emission.

The picture that emerges from detailed calculations of quasar emission line clouds (Kwan and Krolik 1981; Canfield and Puetter 1981; and Netzer 1980) is as follows. There is a more or less classical H II zone which radiates O VI λ1034, C IV λ1549, C III] λ1909, Lyα, etc. This zone is bounded sharply when all the "low" energy continuum photons have been absorbed. Beyond this limit, an extensive partially ionized region exists (ionized fraction ~0.2, $T_e$~8,000 K) which is maintained by the X-ray continuum. This region, where essentially all Fe is Fe II, produces the Balmer lines and continuum, O I λ8446 and collisionally excited Mg II λ2798 and Fe II multiplets. Since this extended partially ionized region is

almost certainly optically thick in the Fe II resonance lines, many of the strong UV Fe II photons which are directly excited by collisional excitation will be transformed after a sufficient number of scatterings into lower transition probability optical Fe II lines.

In this paper, I will present (in § II) an extensive and consistent set of observations of the optical and, principally, the UV Fe II blends in quasars (and a few Seyfert 1 galaxies). Measurements of the hydrogen Balmer lines and continuum, Mg II λ2798, and the power law spectral index are also presented. In § III, these Fe II observations will be compared with the predictions of optically thick collisional excitation models using both the strengths of the blends and comparisons between the observed spectra and synthetic spectra generated from detailed models. From these comparisons, the accuracy of the models will be judged and a likely direction for future theoretical work will be sketched.

## II. OBSERVATIONS AND REDUCTIONS

Spectrophotometric measurements of 38 quasars and Seyfert 1 galaxies will be discussed here. All of the observations were obtained with the Robinson-Wampler image-tube scanner (ITS) (Robinson and Wampler 1972; Miller, Robinson, and Schmidt 1980) mounted on the Lick Observatory 3 m Shane reflector on Mount Hamilton. Many of these observations were taken by other observers for other programs; I thankfully acknowledge contributions of data from M. M. Phillips, J. M. Shuder, J. A. Baldwin, E. J. Wampler, and D. E. Osterbrock.

Individual spectral scans of a particular object cover about 2,400 Å at a resolution of approximately 10 Å. Several scans, covering different wavelength ranges, were taken for each object and reduced using "standard techniques" (Osterbrock 1977). Because of the small entrance aperture used, not to mention occasional less than perfect weather, accurate absolute flux calibrations are impossible to obtain for these scans; but experience has shown that the relative flux calibration within each scan should be accurate to at least 15%. Special precautions were taken for ultraviolet scans to lessen the impact of atmospheric dispersion; a blue filter was often used in front of the TV guiding system, the spectrograph slit was often rotated for alignment with the dispersion direction, and large aperture observations were occasionally used to calibrate the small aperture scans.

The individual scans for each object were "gray-shifted" by suitable constants to align their flux scales (weighted according to signal-to-noise ratio) and combined into a single composite spectrum of up to 6,000 Å in length. Significantly divergent scans were excluded from the composites. Usually, the component scans were taken within a few months of each other, but for some objects, several years elapsed between scans. However, in only two cases (4C 29.45=1156+295 and 3C 120=1430+05; see below) did significant changes occur between observations that invalidated the resulting composite spectra. Finally, the composite spectra were digitally "unredshifted" and placed on a rest wavelength versus relative $F_\lambda$ scale. Examples of these composite spectra are shown in Figure 1, and in Grandi and Phillips (1979, Fig. 1).

The composite spectra were measured to determine various quantities of interest: line strengths and equivalent widths of Balmer lines, Mg II λ2798 and Fe II blends, strength of the Balmer continuum emission, and power law index. Figure 1 illustrates the lines measured. The measurement technique was unsophisticated; a continuum was drawn in by eye, and the limits of each measured line were delineated on this continuum. No attempt was made to completely "deblend" merged lines such as Hβ and [O III] λλ4959, 5007. However, since the goal of the present investigation is not accurate Balmer line ratios, the extra effort needed to accurately determine the Hβ strength did not seem warranted.

The notation used to specify the blended Fe II emission that is observed in quasars and Seyfert 1 galaxies deserves comment. The optical Fe II emission (as discussed in Osterbrock 1977 and Phillips 1978*a*) appears in two prominent blends: λ4570 (consisting of Fe II lines in multiplets 26, 37, 38, 43, and 44) and λλ5190, 5320 (multiplets 42, 48, 49, and 55). Note that He II λ4686 emission, if present, will be included in the measurement of the Fe II λ4570 blend. Usually, however, He II λ4686 is not seen. For the UV Fe II blends, I have used the observations of Wills *et al.* (1980); Wills, Netzer, and Wills (1980); Grandi and Phillips (1980); and the synthetic spectra described below, to create the following notation for the observed blends: λ2100 (called λ2050 by Wills *et al.* 1980), which apparently consists of multiplets UV83, UV93, UV91, and UV90; λ2500 (called λλ2300–2600 by Wills *et al.* 1980), a very broad blend which apparently consists of multiplets UV4, UV3, UV35, UV2, UV34, UV33, UV64, UV1, and possibly others, as well as C II] λ2326; λ2950, which apparently consists of multiplets UV61, UV60 (also known as multiplet 2) and 8; and λ3200, which apparently consists of multiplets 7, 6, and 1. Wills *et al.* (1980) also discuss an Fe II blend near λ2750 which apparently consists of multiplets UV62 and UV63. However, in most objects, this blend is almost inextricably merged with Mg II λ2798. Therefore, even in objects where Fe II λ2750 could be distinguished, the measurement of Mg II λ2798 included λ2750.

The rest frame equivalent widths and fluxes (or conservative upper limits) for the Fe II blends as well as for Mg II λ2798, Hγ, Hβ, and Hα are listed in Table 1 for each of the 38 program objects. The line fluxes are given relative to Mg II λ2798 except where Mg II λ2798 was not observed or was very poorly observed, in which case,

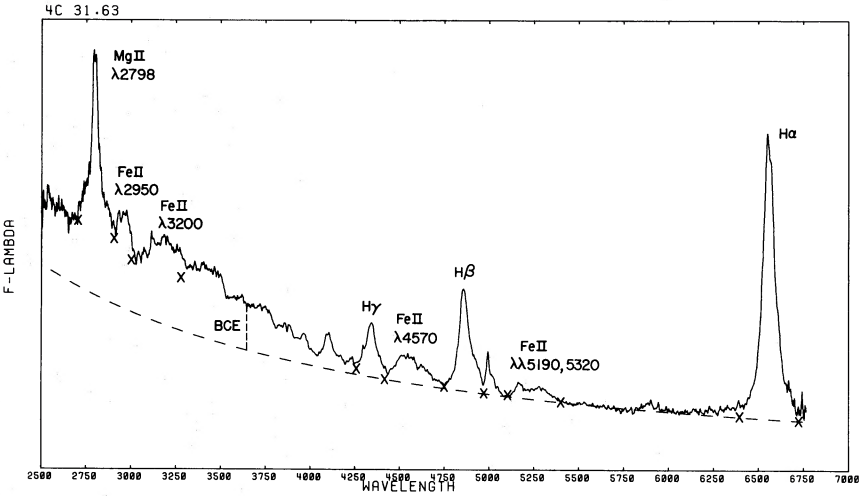


FIG. 1*a*

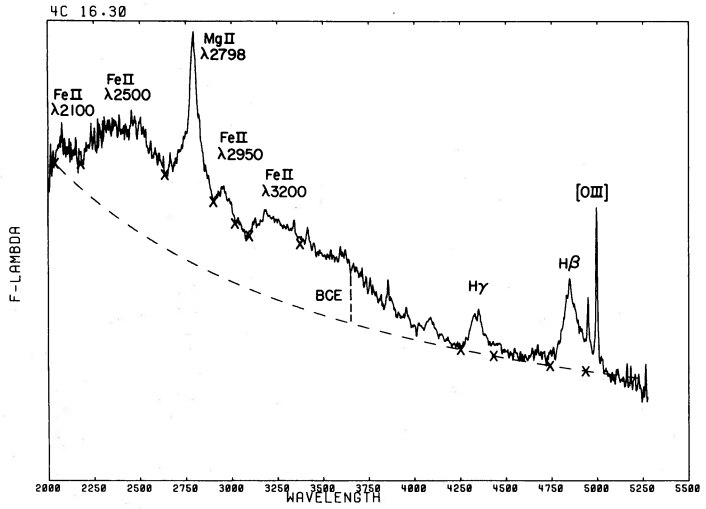


FIG. 1*b*

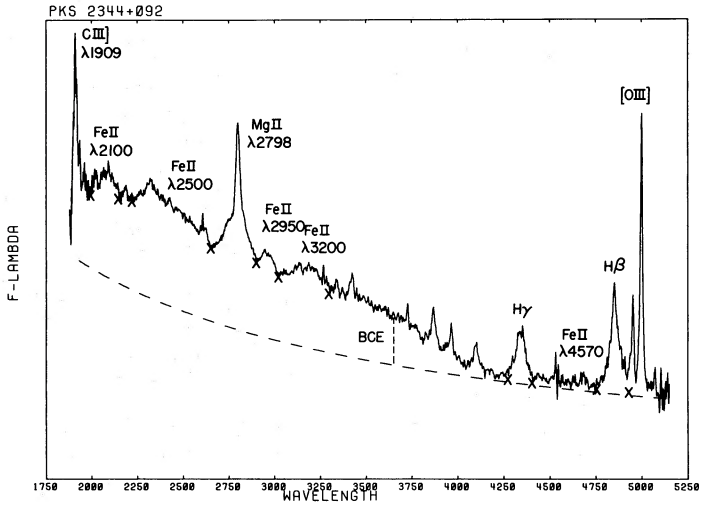


FIG. 1*c*

FIG. 1.—Composite scans of four quasars are plotted on a relative $F_\lambda$ vs. rest wavelength scale. 4C 31.63 is plotted in (*a*), 4C 16.30 is plotted in (*b*), PKS 2344+092 is plotted in (*c*), and PKS 1252+119 is plotted in (*d*). Fitted power laws are shown as dashed lines for 4C 31.63, 4C 16.30, and PKS 2344+092. Crosses show the limits and continuum levels used to measure the various labelled emission lines. The dashed lines marked BCE show the measured Balmer continuum emission. The horizontal axes correspond to zero flux.

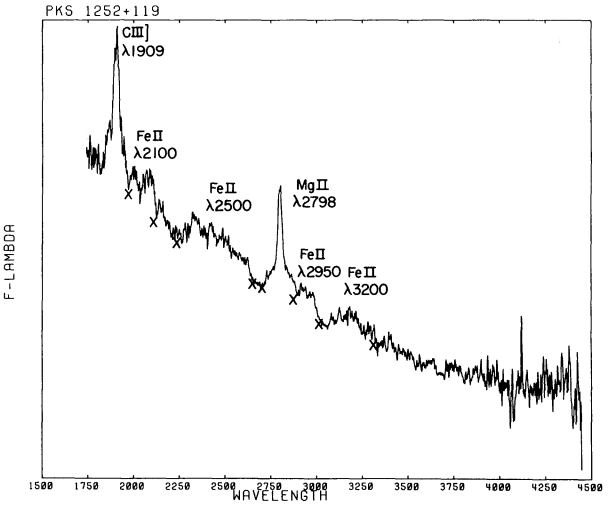


FIG. 1*d*

Hβ was used as the standard. I estimate that the uncertainties in these measurements should be less than 25% for the Mg II and unblended Balmer lines, and less than 50% for the less well defined Fe II blends and the usually badly blended Hβ line. Particularly uncertain measurements are marked with a colon. Also listed in Table 1 are the absolute observed rest frame line fluxes (ergs $cm^{-2}$ $s^{-1}$) for the standard line of each object. Because of the problems discussed above, these absolute fluxes should be treated with caution; I estimate that in some cases, they could be uncertain by up to 100%. For some objects, no absolute calibration was available; these objects are indicated with an entry of NA.

The power law spectral index ($\alpha$) and Balmer continuum integrated flux ($F^{BC}$) measurements contained in Table 1 (for 31 and 28 objects, respectively) were created in the following manner. A power law was fitted by least squares to hand-selected continuum points longward of λ4250. This power law can be expressed in terms of $F_\lambda$ as:

$$F_\lambda = K_1 \lambda^{\alpha-2},$$

or, as is more familiar, in terms of $F_\nu$:

$$F_\nu = K_2 \nu^{-\alpha}.$$

See Figure 1 for examples of fitted power laws. The power law was then subtracted from the entire composite scan. Examples of such power law subtracted scans are shown in Grandi and Phillips (1980, Fig. 1). From the power law subtracted scans, the value of $F_\lambda^{BE}$ at the wavelength of the Balmer edge ($\lambda^{BE}$) was measured and assumed to be due solely to (optically thin) Balmer continuum emission. The measured value of $F_\lambda^{BE}$ was converted into a value for the integrated flux in the Balmer continuum ($F^{BC}$, which is expressed relative to Mg II λ2798 or Hβ) by using the relation:

$$F^{BC} = \int_0^{\lambda_{BE}} F_\lambda^{BC}\, d\lambda = F_\lambda^{BE} \frac{(\lambda_{BE})^2}{c} \frac{(kT_e)}{h}.$$

A value of 10,000 K for the electron temperature ($T_e$) was chosen. For three objects (3C 48, PKS 1510−089, and Mrk 854), no emission was apparent at the Balmer edge after the power law was removed. Based on comparisons of measurements of $\alpha$ and $F^{BC}$ from independent composite scans of the same object, I estimate that the uncertainties in $\alpha$ and $F^{BC}$ should be roughly 25%. Of course, for objects with little observed continuum longward of λ4250, the values of $\alpha$ and $F^{BC}$ will be more uncertain. Also, since optically thin Balmer continuum emission is unlikely to be the sole contributor to the emission shortward of the Balmer edge, the so-called "λ3000 bump," discussed in Grandi (1982), the theoretical interpretation of the measured $F^{BC}$ values is likely to be complicated.

Measurements of many of the objects discussed here have been reported elsewhere in the literature. In particular, completely independent observations of 4C 34.47 are discussed by Soifer *et al.* (1981); 4C 31.63 and 3C 273 by Puetter *et al.* (1981); 3C 380 and 3C 454.3 by Wills *et al.* (1980); 3C 48, 3C 232, 3C 273, PKS 1510−089, 3C 351, 4C 31.63, and 3C 454.3 by Neugebauer *et al.* (1979); and 4C 31.63, B2 0738+313 and PKS 2344+092 by Richstone and Schmidt (1980). Several papers have included measurements and analyses based on some of the same Lick Observatory ITS data scans that have been incorporated into the composite scans measured here. These papers include Baldwin (1975*a*, *b*, 1977), Osterbrock (1977), Phillips (1977, 1978*a*), and Grandi and Phillips (1979, 1980). However, many new scans have been added to the "data library" since these papers were written, sometimes completely superseding the earlier data (the dates of observation are listed in Table 1 for each object). Generally, the agreement between measurements reported here and in the above-mentioned papers is within the uncertainties discussed earlier. I would advise, however, that Balmer line measurements contained in the earlier Lick papers should be used instead of the values reported here given the lack of sophistication used in the present measurements. Another germane comparison to previous work is that for four objects (4C 61.20, 3C 57, 3C 380, and PKS 2344+092) measured by Phillips (1978*a*) to have no emission at Fe II λ4570, I have concluded that λ4570 emission does in fact exist.

As noted above, significant line and continuum variability was noted between scans taken over a period of several years for two objects. One of these objects is the familiar Seyfert 1 galaxy 3C 120. French and Miller (1980) have discussed the line variability of this object.

TABLE 1

OBSERVATIONS OF QUASARS AND SEYFERT 1 GALAXIES

| VARIABLE | Mrk 335 0003+199 11/74, 12/75 11/76, 1/77 | | PKS 0044+030 0044+030 1/77, 7/78 | | PHL 959 0100+020 12/80 | | 3C 48 0134+329 9/76, 11/76 | | PKS 0155−109 0155−109 10/74, 11/74 8/75 | | 3C 57 0159−117 10/78 | |
|---|---|---|---|---|---|---|---|---|---|---|---|---|
| | $F$ | $W_\lambda$ | $F$ | $W_\lambda$ | $F$ | $W_\lambda$ | $F$ | $W_\lambda$ | $F$ | $W_\lambda$ | $F$ | $W_\lambda$ |
| Fe II λ2100 | ... | ... | ... | ... | ... | ... | ... | ... | ... | ... | ... | ... |
| Fe II λ2500 | ... | ... | ... | ... | ... | ... | ... | ... | 1.4 | 61. | ... | ... |
| Mg II λ2798 | ... | ... | 1.0 | 52. | 1.0 | 67. | 1.0 | 34. | 1.0 | 45. | 1.0 | 25. |
| Fe II λ2950 | ... | ... | 0.18 | 10. | 0.12 | 9.4 | 0.46 | 17. | 0.21 | 10. | 0.23 | 6.6 |
| Fe II λ3200 | ... | ... | 0.23 | 15. | 0.24 | 19. | 0.43 | 16. | 0.71 | 40. | 0.25 | 8.8 |
| Hγ λ4340 | 0.56 | 58. | 0.29 | 42. | 0.17 | 32. | 0.77 | 45. | 0.62 | 88. | 0.31 | 23. |
| Fe II λ4570 | 0.82 | 95. | 0.25 | 41. | 0.16 | 34. | 0.99 | 63. | <0.72 | <120. | 0.55 | 45. |
| Hβ λ4861 | 1.0 | 125. | 0.56 | 102. | 0.30 | 67. | 1.0 | 69. | 1.0 | 204. | 0.62 | 56. |
| Fe II λλ5190, 5320 | 0.49 | 67. | ... | ... | ... | ... | 1.0 | 77. | ... | ... | ... | ... |
| Hα λ6563 | 3.1 | 475. | ... | ... | ... | ... | ... | ... | ... | ... | ... | ... |
| Balmer Cont. | 7.3 | | 2.6 | | 2.4 | | ... | | 2.1 | | 3.0 | |
| $F^{obs}_{Mg\ II}$ (ergs cm$^{-2}$ s$^{-1}$) | ... | | $8.2\times10^{-14}$ | | NA | | $4.7\times10^{-14}$ | | NA | | $4.0\times10^{-14}$ | |
| $F^{obs}_{H\beta}$ | $8.6\times10^{-13}$ | | ... | | ... | | ... | | ... | | ... | |
| $z$ | 0.0257 | | 0.624 | | 0.395 | | 0.367 | | 0.616 | | 0.669 | |
| $\alpha$ | 1.13 | | 0.18 | | 0.17 | | 0.61 | | 0.03 | | 0.29 | |

| VARIABLE | PKS 0414−060 0414−060 10/78 | | Mrk 9 0732+589 10/76, 11/76 4/77 | | PKS 0736+017 0736+017 12/71→10/73, 11/76 | | B2 0738+313 0738+313 1/77 | | PG 0953+415 0953+415 4/80, 6/80 | | 3C 232 0955+326 3/77, 4/80 | |
|---|---|---|---|---|---|---|---|---|---|---|---|---|
| | $F$ | $W_\lambda$ | $F$ | $W_\lambda$ | $F$ | $W_\lambda$ | $F$ | $W_\lambda$ | $F$ | $W_\lambda$ | $F$ | $W_\lambda$ |
| Fe II λ2100 | ... | ... | ... | ... | ... | ... | ... | ... | ... | ... | ... | ... |
| Fe II λ2500 | 0.37: | 14.: | ... | ... | ... | ... | 0.76 | 40. | ... | ... | 0.32 | 14. |
| Mg II λ2798 | 1.0 | 47. | ... | ... | 1.0 | 62. | 1.0 | 60. | 1.0 | 37. | 1.0 | 47. |
| Fe II λ2950 | 0.12 | 6.4 | ... | ... | 0.22 | 14. | 0.18 | 12. | 0.11 | 4.2 | 0.23 | 12. |
| Fe II λ3200 | 0.28 | 17. | ... | ... | 0.59 | 38. | 0.28 | 22. | 0.30 | 13. | 0.18 | 12. |
| Hγ λ4340 | 0.21 | 27. | 0.44 | 44. | 0.44 | 44. | 0.24 | 48. | 0.35 | 35. | 0.097 | 11. |
| Fe II λ4570 | <0.29 | <41. | 0.63 | 67. | 0.57 | 62. | 0.39 | 87. | 0.42 | 49. | 0.56: | 68.: |
| Hβ λ4861 | 0.56: | 86.: | 1.0 | 111. | 0.79 | 91. | 0.45 | 111. | 0.86 | 115. | 0.21 | 28. |
| Fe II λλ5190, 5320 | ... | ... | 0.42 | 50. | 0.27 | 34. | ... | ... | 0.17 | 26. | ... | ... |
| Hα λ6563 | ... | ... | 2.9 | 405. | 2.5 | 374. | ... | ... | 2.6 | 477. | ... | ... |
| Balmer cont. | 3.9 | | 4.9 | | 4.4 | | 3.2 | | 11.4: | | 2.1 | |
| $F^{obs}_{Mg\ II}$ (ergs cm$^{-2}$ s$^{-1}$) | $7.2\times10^{-14}$ | | ... | | $5.7\times10^{-14}$ | | $9.2\times10^{-14}$ | | $2.2\times10^{-13}$ | | $7.1\times10^{-14}$ | |
| $F^{obs}_{H\beta}$ | ... | | $2.1\times10^{-12}$ | | ... | | ... | | ... | | ... | |
| $z$ | 0.781 | | 0.039 | | 0.191 | | 0.630 | | 0.234 | | 0.533 | |
| $\alpha$ | 0.66 | | 1.37 | | 1.09 | | 0.21 | | 1.99 | | 1.12 | |

The other object is 4C 29.45=1156+295. Between ITS scans taken in 1977 April and 1979 May, the rest frame equivalent of Mg II λ2798 dropped by a factor of 4 from 54 Å to 14 Å, while the Mg II λ2798 line flux stayed constant within 25% (a reasonable estimate for the observational error). In 1980 December, another ITS scan (with no absolute flux calibration) was taken of 4C 29.45 with essentially the same equivalent width of Mg II λ2798 as the 1979 May scan.

### III. Fe II EMISSION AND SYNTHETIC SPECTRA

From program objects with well observed Mg II λ2798 emission, the mean line ratio values listed in Table 2 were calculated. Because of this insistence on Mg II observations, all of the objects analyzed for Table 2 are quasars, rather than Seyfert 1 galaxies, with the probable exceptions of Mrk 64 and Mrk 830. The mean line ratios agree well with the mean line ratios determined from the measurements of Wills *et al.* (1980) for Fe II λ2100, λ2500, and λ2950 (0.27, 0.91, and 0.12 respectively) and Phillips (1978*a*) for Fe II λ4570 (0.45, using a value of Mg II λ2798/Hβ=1.60 as determined by Grandi and Phillips 1980). One note must be appended to Table 2: several objects show no Fe II λ4570, have only conservative upper limits shown in Table 1, and are excluded from the λ4570/Mg II λ2798 ratio. Conse-

TABLE 1—*Continued*

| Variable | 4C 06.41 1038+064 3/79 | | 4C 61.20 1049+616 4/77, 5/79 | | 4C 16.30 1104+167 1/77, 2/80 4/80 | | MC2 1215+113 1215+113 3/79 | | 3C 273 1226+023 3/76, 4/76 6/76 | | PKS 1252+119 1252+12 4/77, 2/80, 4/80 | |
|---|---|---|---|---|---|---|---|---|---|---|---|---|
| | $F$ | $W_\lambda$ | $F$ | $W_\lambda$ | $F$ | $W_\lambda$ | $F$ | $W_\lambda$ | $F$ | $W_\lambda$ | $F$ | $W_\lambda$ |
| Fe II λ2100 | 0.42 | 5.6 | ... | ... | 0.20: | 8.4: | 0.36 | 8.3 | ... | ... | 0.37 | 9.2 |
| Fe II λ2500 | 1.3: | 24.: | ... | ... | 1.1 | 56. | 1.1 | 32. | ... | ... | 1.4 | 46. |
| Mg II λ2798 | 1.0 | 23. | 1.0 | 41. | 1.0 | 47. | 1.0 | 38. | 0.44: | 17.: | 1.0 | 38. |
| Fe II λ2950 | 0.18: | 4.4: | 0.17 | 7.5 | 0.20 | 10. | 0.34 | 15. | 0.22 | 8.5 | 0.31 | 13. |
| Fe II λ3200 | 0.51: | 16.: | 0.52 | 24. | 0.37 | 21. | ... | ... | 0.71 | 28. | 0.67 | 33. |
| Hγ λ4340 | ... | ... | 0.32 | 31. | 0.34 | 38. | ... | ... | 0.38 | 26. | ... | ... |
| Fe II λ4570 | ... | ... | 0.32 | 34. | <0.36 | <44. | ... | ... | 0.35 | 26. | ... | ... |
| Hβ λ4861 | ... | ... | 0.57 | 67. | 0.73 | 97. | ... | ... | 1.0 | 84. | ... | ... |
| Fe II λλ5190 5320 | ... | ... | ... | ... | ... | ... | ... | ... | 0.52 | 50. | ... | ... |
| Hα λ6563 | ... | ... | ... | ... | ... | ... | ... | ... | 4.3 | 557. | ... | ... |
| Balmer cont. | ... | | 3.0 | | 4.7 | | ... | | 2.0 | | ... | |
| $F^{obs}_{Mg\ II}$ (ergs cm$^{-2}$ s$^{-1}$) | NA | | $4.2\times10^{-14}$ | | $7.5\times10^{-14}$ | | NA | | ... | | $3.1\times10^{-14}$ | |
| $F^{obs}_{H\beta}$ | ... | | ... | | ... | | ... | | $1.6\times10^{-12}$ | | ... | |
| $z$ | 1.270 | | 0.422 | | 0.634 | | 1.396 | | 0.158 | | 0.871 | |
| $\alpha$ | ... | | 0.17 | | 0.95 | | ... | | 0.48 | | ... | |

| Variable | B 201 1257+346 3/79 | | Mrk 64 1304+346 1/77, 4/78, 12/80 | | Ton 153 1317+277 5/79, 6/79 2/80 | | Mrk 478 1440+356 1/76, 3/76, 4/76 | | Mrk 830 1449+589 5/78, 6/78, 7/78 | | 3C 309.1 1458+718 7/77, 8/78 | |
|---|---|---|---|---|---|---|---|---|---|---|---|---|
| | $F$ | $W_\lambda$ | $F$ | $W_\lambda$ | $F$ | $W_\lambda$ | $F$ | $W_\lambda$ | $F$ | $W_\lambda$ | $F$ | $W_\lambda$ |
| Fe II λ2100 | 0.20 | 5.8 | ... | ... | 0.53 | 8.2 | ... | ... | ... | ... | 0.12: | 10.: |
| Fe II λ2500 | 0.69 | 25. | ... | ... | 0.95 | 18. | ... | ... | ... | ... | 1.3 | 116. |
| Mg II λ2798 | 1.0 | 39. | 1.0 | 74. | 1.0 | 22. | ... | ... | 1.0 | 61. | 1.0 | 97. |
| Fe II λ2950 | 0.25 | 11. | 0.24 | 20. | 0.26 | 6.6 | ... | ... | 0.048 | 3.0 | 0.13 | 14. |
| Fe II λ3200 | 0.54 | 26. | 0.47 | 42. | 0.61 | 18. | 1.1: | 47.: | 0.25 | 18. | 0.35 | 45. |
| Hγ λ4340 | ... | ... | 0.13 | 23. | ... | ... | 0.84 | 64. | 0.16 | 26. | ... | ... |
| Fe II λ4570 | ... | ... | 0.45 | 83. | ... | ... | 1.0 | 84. | 0.32 | 56. | ... | ... |
| Hβ λ4861 | ... | ... | 0.60 | 119. | ... | ... | 1.0 | 90. | 0.45 | 87. | ... | ... |
| Fe II λλ5190 5320 | ... | ... | <0.42 | <86. | ... | ... | 1.0 | 96. | 0.12 | 26. | ... | ... |
| Hα λ6563 | ... | ... | 1.4 | 236. | ... | ... | 4.0 | 412. | 1.4 | 348. | ... | ... |
| Balmer cont. | ... | | 4.6 | | ... | | 6.6 | | 2.5 | | ... | |
| $F^{obs}_{Mg\ II}$ (erg cm$^{-2}$ s$^{-1}$) | NA | | $6.8\times10^{-14}$ | | $3.1\times10^{-14}$ | | ... | | $1.1\times10^{-13}$ | | $3.8\times10^{-14}$ | |
| $F^{obs}_{H\beta}$ | ... | | ... | | ... | | $2.2\times10^{-13}$ | | ... | | ... | |
| $z$ | 1.375 | | 0.189 | | 1.02 | | 0.0773 | | 0.210 | | 0.905 | |
| $\alpha$ | ... | | 2.02 | | ... | | 1.68 | | 1.13 | | ... | |

quently, while all the quasars in the sample seem to have roughly equal UV Fe II blend strengths, some of them have significantly less (or none at all) optical Fe II emission. This curiosity was first pointed out by Phillips (1977, 1978*a*) who noted that most of the quasars he observed were lacking in optical Fe II emission as compared to his Seyfert 1 galaxies. From the present sample of objects, I would modify Phillips's conclusion in two ways. First, *all* quasars apparently show UV Fe II emission, and second, perhaps only 25% of the quasars lack optical Fe II emission (note, from above, that I seem more generous in identifying λ4570 in quasars than Phillips). In the majority of quasars, however, Fe II λ2500/Fe II λ4570 ~ 2. A possible interpretation of this distinction is that quasars that have optically *thin* Fe II regions do not show optical Fe II emission (see below).

There have been several recent attempts, of varying degrees of complexity, to model collisionally excited, optically thick Fe II emission in quasars and Seyfert 1 galaxies. Phillips (1978*b*) calculated several such models using a 25 level atom (consisting of 16 terms) with 413 lines in 78 multiplets (including some downward transitions to levels not among the 25 in the model). Unfortunately, none of the eight eV terms which apparently give rise to the λ2100 blend, nor the low-lying doublet terms which can feed some of these eight eV levels, were

TABLE 1—*Continued*

| Variable | PKS 1510−089 1510−089 5/76, 6/76, 7/76 | | Mrk 854 1524+436 5/78, 6/78 | | Mrk 876 1613+658 4/80, 6/80 | | PKS 1656+053 1656+053 5/79, 6/79 | | 3C 351 1704+608 4/80, 6/80 | | 4C 34.47 1721+343 6/76, 4/78 | |
|---|---|---|---|---|---|---|---|---|---|---|---|---|
| | $F$ | $W_\lambda$ | $F$ | $W_\lambda$ | $F$ | $W_\lambda$ | $F$ | $W_\lambda$ | $F$ | $W_\lambda$ | $F$ | $W_\lambda$ |
| Fe II λ2100 | ... | ... | ... | ... | ... | ... | ... | ... | ... | ... | ... | ... |
| Fe II λ2500 | ... | ... | ... | ... | ... | ... | 1.3 | 44. | ... | ... | ... | ... |
| Mg II λ2798 | 1.0 | 55. | ... | ... | 1.2: | 44.: | 1.0 | 37. | 1.0 | 41. | 1.0 | 115. |
| Fe II λ2950 | 0.16 | 10. | ... | ... | 0.30 | 12. | 0.37 | 15. | 0.12 | 5.3 | 0.05 | 6.1 |
| Fe II λ3200 | 0.37 | 26. | 1.1: | 48.: | 0.95 | 43. | 0.72 | 32. | 0.42 | 20. | 0.30 | 37. |
| Hγ λ4340 | 0.42 | 38. | 0.80 | 64. | 0.45 | 42. | ... | ... | 0.16 | 13. | 0.23 | 76. |
| Fe II λ4570 | 0.42 | 39. | 1.4 | 115. | 0.48 | 50. | ... | ... | 0.49 | 43. | 0.16 | 58. |
| Hβ λ4861 | 0.76 | 78. | 1.0 | 85. | 1.0 | 114. | ... | ... | 0.30 | 29. | 0.32 | 122. |
| Fe II λλ5190 5320 | 0.50 | 58. | 1.1 | 95. | 0.40 | 51. | ... | ... | 0.56 | 65. | <0.076 | <30. |
| Hα λ6563 | ... | ... | 3.1 | 309. | 5.2 | 792. | ... | ... | ... | ... | 2.1 | 966. |
| Balmer cont. | ... | | ... | | 5.8 | | ... | | 0.94 | | 2.9 | |
| $F^{obs}_{Mg\ II}$ (ergs cm$^{-2}$ s$^{-1}$) | NA | | ... | | ... | | $2.1\times10^{-14}$ | | $6.1\times10^{-14}$ | | $2.3\times10^{-13}$ | |
| $F^{obs}_{H\beta}$ | ... | | $1.6\times10^{-14}$ | | $1.4\times10^{-13}$ | | ... | | ... | | ... | |
| $z$ | 0.361 | | 0.150 | | 0.128 | | 0.879 | | 0.371 | | 0.206 | |
| $\alpha$ | 1.06 | | 1.36 | | 1.00 | | ... | | 1.01 | | 1.10 | |

| Variable | 3C 380 1828+487 11/76, 4/77, 6/80 | | PKS 2128−123 2128−123 10/78 | | II Zw 136 2130+099 6/75, 6/76, 9/76 | | 4C 31.63 2201+315 6/80 | | Mrk 304 2214+139 11/74, 12/74, 11/76 | | 3C 454.3 2251+158 10/78 | |
|---|---|---|---|---|---|---|---|---|---|---|---|---|
| | $F$ | $W_\lambda$ | $F$ | $W_\lambda$ | $F$ | $W_\lambda$ | $F$ | $W_\lambda$ | $F$ | $W_\lambda$ | $F$ | $W_\lambda$ |
| Fe II λ2100 | ... | ... | ... | ... | ... | ... | ... | ... | ... | ... | ... | ... |
| Fe II λ2500 | 0.94 | 56. | ... | ... | ... | ... | ... | ... | ... | ... | 0.93 | 34. |
| Mg II λ2798 | 1.0 | 65. | 1.0 | 70. | ... | ... | 1.0 | 55. | ... | ... | 1.0 | 40. |
| Fe II λ2950 | 0.077 | 5.4 | 0.22 | 16. | ... | ... | 0.26 | 16. | ... | ... | 0.24 | 9.9 |
| Fe II λ3200 | 0.47 | 35. | 0.30 | 24. | ... | ... | 0.33 | 21. | ... | ... | 0.26 | 12. |
| Hγ λ4340 | 0.29 | 48. | 0.33 | 54. | 0.50 | 63. | 0.28 | 37. | 0.43 | 45. | 0.47 | 35. |
| Fe II λ4570 | 0.50 | 96. | <0.27 | <49. | 0.59 | 82. | 0.30 | 42. | 0.57 | 65. | ... | ... |
| Hβ λ4861 | 0.58 | 118. | 0.66 | 129. | 1.0 | 160. | 0.65 | 106. | 1.0 | 121. | ... | ... |
| Fe II λλ5190 5320 | ... | ... | <0.30 | <66. | 0.44 | 83. | 0.21 | 39. | 0.26 | 35. | ... | ... |
| Hα λ6563 | ... | ... | ... | ... | 3.6 | 88.5 | 2.1 | 493. | 3.6 | 555. | ... | ... |
| Balmer cont. | 4.5 | | 4.0 | | 4.0 | | 3.8 | | 4.9 | | 2.5 | |
| $F^{obs}_{Mg\ II}$ (ergs cm$^{-2}$ s$^{-1}$) | $4.3\times10^{-14}$ | | $1.4\times10^{-13}$ | | ... | | $1.4\times10^{-13}$ | | ... | | $2.4\times10^{-14}$ | |
| $F^{obs}_{H\beta}$ | ... | | ... | | $3.4\times10^{-13}$ | | ... | | $6.1\times10^{-13}$ | | ... | |
| $z$ | 0.692 | | 0.501 | | 0.062 | | 0.297 | | 0.0661 | | 0.859 | |
| $\alpha$ | 1.47 | | 1.03 | | 0.49 | | 0.60 | | 0.79 | | 1.39 | |

included in the model atom. Phillips considered a uniform temperature and density spherical cloud consisting entirely of Fe II. All the collisional excitations were assumed to occur at cloud center, and a mean escape probability formalism was used to approximate the scattering of line photons out of the cloud. The free parameters in these models were the electron temperature ($T_e$) and the line center optical depth in the λ2344 component of multiplet UV3 ($\tau_{\lambda 2344}$). No attempt was made to predict the Fe II strengths compared to Mg II λ2798 or Hβ; only relative Fe II strengths could be determined. For lack of anything better, collisional excitation rates were approximately calculated using the formula of van Regemorter (1962) for permitted transitions. However, an extensive set of transition probabilities (Phillips 1979) was collected for the model calculations. Phillips's goal was to reproduce the relative strengths found in the λ4570 and λλ5190, 5320 blends in the narrow line Fe II galaxy I Zw 1. He found a model with $T_e = 15{,}000$ K and $\tau_{\lambda 2344} = 5000$ gave a quite good fit to the λ4570 blend and a not so good fit to the λλ5190, 5320 blend.

Phillips has kindly supplied me with a detailed listing of a model with parameters $T_e = 10{,}000$ K and $\tau_{\lambda 2344} = 5000$. Relevant relative Fe II blend ratios are listed in Table 3 (using the multiplet identifications for each blend as described above) and total multiplet strengths (relative to UV2) are listed in Table 4 (the wavelength listed is an intensity weighted mean of the individual components).

TABLE 1—*Continued*

| Variable | 4C 09.72 2308+098 10/78 | | PKS 2344+092 2344+092 8/74→8/75, 9/76 | |
|---|---|---|---|---|
| | $F$ | $W_\lambda$ | $F$ | $W_\lambda$ |
| Fe II λ2100 | ... | ... | 0.33 | 10. |
| Fe II λ2500 | ... | ... | 0.83 | 28. |
| Mg II λ2798 | 5.2: | 67.: | 1.0 | 40. |
| Fe II λ2950 | 0.71: | 10.: | 0.15 | 6.4 |
| Fe II λ3200 | 0.60 | 11. | 0.39 | 18. |
| Hγ λ4340 | 0.35 | 16. | 0.51 | 47. |
| Fe II λ4570 | 0.42: | 22.: | 0.45 | 46. |
| Hβ λ4861 | 1.0 | 58. | 0.86 | 94. |
| Fe II λλ5190 5320 | ... | ... | ... | ... |
| Hα λ6563 | ... | ... | ... | ... |
| Balmer cont. | 4.7 | | 5.8 | |
| $F^{obs}_{Mg\ II}$ (ergs cm$^{-2}$ s$^{-1}$) | ... | | $6.9\times10^{-14}$ | |
| $F^{obs}_{H\beta}$ | $1.0\times10^{-13}$ | | ... | |
| $z$ | 0.432 | | 0.677 | |
| $\alpha$ | −0.15 | | 1.57 | |

TABLE 2

Fe II Observed Mean Blend Ratios

| Ratio | Mean | Standard Deviation | Number of Objects | Range |
|---|---|---|---|---|
| λ2100/Mg II λ2798 | 0.32 | 0.13 | 8 | 0.12→0.53 |
| λ2500/Mg II λ2798 | 0.98 | 0.34 | 15 | 0.37→1.4 |
| λ2950/Mg II λ2798 | 0.20 | 0.09 | 28 | 0.05→0.46 |
| λ3200/Mg II λ2798 | 0.41 | 0.15 | 28 | 0.18→0.71 |
| λ4570/Mg II λ2798 | 0.43 | 0.19 | 17 | 0.16→0.99 |
| λλ5190, 5320/Mg II λ2798 | 0.40 | 0.31 | 7 | 0.12→1.0 |
| λ2100/λ2500 | 0.33 | ... | ... | ... |
| λ2950/λ2500 | 0.20 | ... | ... | ... |
| λ3200/λ2500 | 0.42 | ... | ... | ... |
| λ4570/λ2500 | 0.44 | ... | ... | ... |
| λλ5190, 5320/λ2500 | 0.41 | ... | ... | ... |
| λ4570/λλ5190, 5320 | 1.1 | ... | ... | ... |

TABLE 3

Fe II Predicted Blend Ratios

| Ratio | Phillips Value | Kwan and Krolik Value |
|---|---|---|
| λ2100/Mg II λ2798 | ... | ... |
| λ2500/Mg II λ2798 | ... | 0.30 |
| λ2950/Mg II λ2798 | ... | 0.074 |
| λ3200/Mg II λ2798 | ... | 0.092 |
| λ4570/Mg II λ2798 | ... | 0.11 |
| λλ5190, 5320/Mg II λ2798 | ... | 0.071 |
| λ2100/λ2500 | ... | ... |
| λ2950/λ2500 | 0.34 | 0.25 |
| λ3200/λ2500 | 0.52 | 0.31 |
| λ4570/λ2500 | 0.12 | 0.35 |
| λλ5190, 5320/λ2500 | 0.13 | 0.24 |
| λ4570/λλ5190, 5320 | 0.91 | 1.5 |

TABLE 4

Fe II PREDICTED MULTIPLET STRENGTHS

| Multiplet | Transition | Mean Wavelength | Phillips Model | Kwan/Krolik Model | Ad Hoc Model |
|---|---|---|---|---|---|
| UV 98 ..... | $a^2G–x^2G^o$ | 1841. | ... | ... | 0.039 |
| UV 97 ..... | $a^2G–y^2F^o$ | 1867. | ... | ... | 0.148 |
| UV 96 ..... | $a^2G–y^2H^o$ | 1931. | ... | ... | 0.078 |
| UV 109 .... | $a^2P–y^2D^o$ | 2059. | ... | ... | 0.086 |
| UV 108 .... | $a^2P–z^2S^o$ | 2095. | ... | ... | 0.086 |
| UV 94 ..... | $a^2G–z^2H^o$ | 2028. | ... | ... | 0.086 |
| UV 93 ..... | $a^2G–y^2G^o$ | 2042. | ... | ... | 0.281 |
| UV 106 .... | $a^2P–z^2P^o$ | 2158. | ... | ... | 0.094 |
| UV 92 ..... | $a^2G–z^2F^o$ | 2070. | ... | ... | 0.062 |
| UV 91 ..... | $a^2G–y^4G^o$ | 2084. | ... | ... | 0.390 |
| UV 66 ..... | $a^4D–x^2D^o$ | 1823. | ... | ... | 0.195 |
| UV 83 ..... | $a^4P–x^4D^o$ | 2014. | ... | ... | 0.382 |
| UV 65 ..... | $a^4D–y^4D^o$ | 1854. | ... | ... | 0.273 |
| UV 90 ..... | $a^2G–z^2G^o$ | 2168. | ... | ... | 0.281 |
| UV 105 .... | $a^2P–z^2D^o$ | 2330. | ... | ... | 0.585 |
| UV 79 ..... | $a^4P–z^4S^o$ | 2166. | ... | ... | 0.039 |
| UV 6 ..... | $a^6D–z^4P^o$ | 2148.6 | 0.047 | 0.057 | 0.047 |
| ... ..... | $a^4F–z^4P^o$ | 2250.7 | 0.049 | ... | 0.049 |
| UV 64 ..... | $a^4D–z^4P^o$ | 2585.2 | 0.061 | 0.107 | *0.919* |
| 8..... | $a^4P–z^4P^o$ | 2983.1 | 0.057 | 0.050 | *0.567* |
| 16..... | $a^2P–z^4P^o$ | 3472.6 | 0.031 | ... | 0.031 |
| 23..... | $a^2D–z^4P^o$ | 3804.8 | 0.0034 | ... | 0.0034 |
| 29..... | $b^4P–z^4P^o$ | 3869.0 | 0.0033 | 0.057 | 0.0033 |
| 39..... | $b^4F–z^4P^o$ | 4129.7 | 0.0005 | 0.014 | 0.0005 |
| 45..... | $a^6S–z^4P^o$ | 4211.8 | 0.0045 | 0.079 | 0.0045 |
| 54..... | $b^2P–z^4P^o$ | 4753.5 | 0.0002 | ... | 0.0002 |
| 74..... | $b^4D–z^4P^o$ | 6346.9 | 0.029 | 0.221 | 0.029 |
| UV 5 ..... | $a^6D–z^4D^o$ | 2260.6 | 0.075 | 0.064 | 0.075 |
| UV 36 ..... | $a^4F–z^4D^o$ | 2381.0 | 0.088 | 0.086 | 0.088 |
| UV 63 ..... | $a^4D–z^4D^o$ | 2750.8 | 0.096 | 0.114 | 0.096 |
| 6..... | $a^4P–z^4D^o$ | 3199.1 | 0.114 | 0.064 | *0.569* |
| 14..... | $a^2P–z^4D^o$ | 3780.5 | 0.0087 | ... | 0.0087 |
| 21..... | $a^2D–z^4D^o$ | 4188.4 | 0.0035 | ... | 0.0035 |
| 27..... | $b^4P–z^4D^o$ | 4278.2 | 0.135 | 0.236 | 0.135 |
| 33..... | $a^4H–z^4D^o$ | 4364.7 | 0.0011 | ... | 0.0011 |
| 38..... | $b^4F–z^4D^o$ | 4565.0 | 0.121 | 0.271 | 0.121 |
| 43..... | $a^6S–z^4D^o$ | 4717.4 | 0.014 | 0.129 | 0.014 |
| 48..... | $a^4G–z^4D^o$ | 5349.9 | 0.054 | 0.186 | 0.054 |
| 73..... | $b^4D–z^4D^o$ | 7575.5 | 0.010 | 0.221 | 0.010 |
| UV 4 ..... | $a^6D–z^4F^o$ | 2260.6 | 0.124 | 0.136 | 0.124 |
| UV 35 ..... | $a^4F–z^4F^o$ | 2369.4 | 0.126 | 0.157 | 0.126 |
| UV 62 ..... | $a^4D–z^4F^o$ | 2734.7 | 0.104 | 0.157 | 0.104 |
| 7..... | $a^4P–z^4F^o$ | 3180.0 | 0.098 | 0.114 | *0.492* |
| 10..... | $a^2G–z^4F^o$ | 3498.4 | 0.0035 | ... | 0.0035 |
| 15..... | $a^2P–z^4F^o$ | 3741.8 | 0.0006 | ... | 0.0006 |
| 28..... | $b^4P–z^4F^o$ | 4203.7 | 0.061 | 0.293 | 0.061 |
| 32..... | $a^4H–z^4F^o$ | 4363.5 | 0.022 | ... | 0.022 |
| 37..... | $b^4F–z^4F^o$ | 4586.7 | 0.161 | 0.529 | 0.161 |
| 44..... | $a^6S–z^4F^o$ | 4663.7 | 0.002 | 0.114 | 0.002 |
| 49..... | $a^4G–z^4F^o$ | 5293.8 | 0.148 | 0.379 | 0.148 |
| 53..... | $b^2P–z^4F^o$ | 5293.1 | 0.0001 | ... | 0.0001 |
| 55..... | $b^2H–z^4F^o$ | 5526.6 | 0.018 | 0.121 | 0.018 |
| 57..... | $a^2F–z^4F^o$ | 5752.6 | 0.0005 | ... | 0.0005 |
| 72..... | $b^4D–z^4F^o$ | 7621.1 | 0.0028 | 0.071 | 0.0028 |
| UV 3 ..... | $a^6D–z^6P^o$ | 2350.9 | 0.158 | 0.250 | 0.158 |
| UV 34 ..... | $a^4F–z^6P^o$ | 2465.4 | 0.119 | 0.193 | *0.954* |
| UV 61 ..... | $a^4D–z^6P^o$ | 2885.9 | 0.228 | 0.279 | 0.228 |
| 5..... | $a^4P–z^6P^o$ | 3408.5 | 0.037 | 0.243 | 0.037 |
| 26..... | $b^4P–z^6P^o$ | 4556.2 | 0.022 | 0.343 | 0.022 |
| 36..... | $b^4F–z^6P^o$ | 4974.7 | 0.023 | 0.329 | 0.023 |
| 42..... | $a^6S–z^6P^o$ | 5052.4 | 0.131 | 0.243 | 0.131 |

TABLE 4—*Continued*

| Multiplet | Transition | Mean Wavelength | Phillips Model | Kwan/Krolik Model | Ad Hoc Model |
|---|---|---|---|---|---|
| 47..... | $a^4G$–$z^6P^o$ | 5894.3 | 0.0004 | 0.0070 | 0.0004 |
| ... ..... | $b^4D$–$z^6P^o$ | 8802.1 | 0.0005 | ... | 0.0005 |
| UV 2 ..... | $a^6D$–$z^6F^o$ | 2385.0 | 1.00 | 1.00 | 1.00 |
| UV 33 ..... | $a^4F$–$z^6F^o$ | 2518.5 | 0.229 | 0.714 | *0.915* |
| UV 60/2 ... | $a^4D$–$z^6F^o$ | 2937.7 | 0.615 | 0.643 | *1.23* |
| 4..... | $a^4P$–$z^6F^o$ | 3480.8 | 0.066 | 0.721 | 0.066 |
| 25..... | $b^4P$–$z^6F^o$ | 4757.7 | 0.012 | 0.571 | 0.012 |
| 30..... | $a^4H$–$z^6F^o$ | 4834.7 | 0.019 | ... | 0.019 |
| 35..... | $b^4F$–$z^6F^o$ | 5160.3 | 0.080 | 0.400 | 0.080 |
| 41..... | $a^6S$–$z^6F^o$ | 5277.5 | 0.052 | 0.679 | 0.052 |
| 46..... | $a^4G$–$z^6F^o$ | 6024.9 | 0.026 | 0.229 | 0.026 |
| UV 1 ..... | $a^6D$–$z^6D^o$ | 2614.6 | 0.796 | 1.38 | 0.796 |
| UV 32 ..... | $a^4F$–$z^6D^o$ | 2742.1 | 0.603 | 1.20 | 0.603 |
| 1..... | $a^4D$–$z^6D^o$ | 3281.0 | 1.14 | 1.04 | *0.571* |
| 3..... | $a^4P$–$z^6D^o$ | 3951.8 | 0.065 | 1.57 | 0.065 |
| 24..... | $b^4P$–$z^6D^o$ | 5720.0 | 0.0015 | 0.043 | 0.0015 |
| 34..... | $b^4F$–$z^6D^o$ | 6233.9 | 0.0033 | 0.179 | 0.0033 |
| 40..... | $a^6S$–$z^6D^o$ | 6479.3 | 0.051 | 0.750 | 0.051 |

Comparing these values with the observed values contained in Table 2 demonstrates that the optical Fe II multiplets are predicted to be much weaker relative to the UV multiplets than observed, although the relative strengths of the two optical blends and of the UV blends are predicted correctly, perhaps indicating that $\tau_{\lambda 2344}$ should be increased.

Two other sets of calculations of Fe II strengths were performed by Collin-Souffrin *et al.* (1979, 1980) and by Netzer (1980) (see also Boksenberg and Netzer 1977). Both calculations treat the case of Fe II and Mg II in the extended transition region of a photoionized slab. Collin-Souffrin *et al.* solved simultaneously the statistical equilibrium and radiative transfer equations for their nine term model atom, while Netzer used a local escape probability formalism to solve the radiative transfer problem for his six term atom in the context of a complete quasar emission region model. Both of these approximations should be superior to the technique used by Phillips, but Phillips solved a considerably more complex atom and he also predicted individual line strengths rather than merely multiplet strengths.

Collin-Souffrin *et al.* made models for many combinations of free parameters ($N_e$, $T_e$, and $\tau_{UV3}$; the line center optical depth for the combined UV3 multiplet) and concluded that values of $T_e \sim 5$–$10 \times 10^3$ K and $\tau_{UV3} \sim 10^5$ were necessary to explain the observations. Collin-Souffrin *et al.* predicted only a few multiplets in comparison to Phillips's models; but, assuming that the λ4570 blend consists solely of multiplets 26, 27, and 38, and the λλ5190, 5320 blend consists solely of multiplets 42, 48, and 49, they predict Fe II λ4570/Mg II λ2798 = 0.58, Fe II λ5190, 5320/Mg II λ2798 = 1.2 and Fe II λ4570/Fe II λλ5190, 5320 = 0.48 for a model with parameters $T_e = 10^4$ K, $N_e = 10^{10}$ cm$^{-3}$, and $\tau_{UV3} = 7 \times 10^4$. These ratios are in reasonable agreement with the observations.

Netzer calculated only a few models, and he predicted strengths for only a few multiplets. One model resulted in $\tau_{UV3} = 395$, $T_e \sim 10^4$ K, $N_e \sim 10^9$ cm$^{-3}$ and predicted (assuming λ2950 consists solely of UV60) Fe II λ2950/Mg II λ2798 = 0.1, and Fe II λ4570/Mg II λ2798 ~0.1 (assuming that Fe II λ4570 is four times the strength of multiplet 42). Again, the agreement with the observations is tolerable.

Kwan and Krolik (1981) (see also Kwan and Krolik 1979) calculated Fe II line strengths in the context of a very complete model of a quasar emission line cloud. A 16 term model Fe II atom was solved simultaneously with all other atomic species in a photoionized slab using local escape probabilities to solve the radiative transfer problem and including escape of line photons from both sides of the slab. Kwan and Krolik considered the same 16 terms of Fe II as Phillips, but since the individual levels in each term were lumped together, only total multiplet strengths were calculated (under the assumption that all the components of each multiplet were optically thick). They used the same transition probability values as Phillips (1979), but somewhat different collisional rates were used. The Fe II blend strengths emerging from Kwan and Krolik's standard model (which has $T_e \sim 8000$ K and $N_e \sim 10^9$ cm$^{-3}$ in the extended transition zone and an approximate value of $\tau_{\lambda 2344} \sim 10^5$) are listed in Table 3 and the multiplet strengths are listed in Table 4.

A debatable facet of Kwan and Krolik's model is their determination of the total slab depth and the sensitivity of their Fe II strengths to this parameter. Kwan and Krolik adjust the column density of their slab so the strength of C II] λ2326 achieves a certain value.

This procedure is rather arbitrary (presumably the extended ionization region could be made almost indefinitely large depending on the postulated X-ray continuum) and ignores physical effects which might provide a natural limit to the emission slab size (for example, the radiative acceleration mechanism of Blumenthal and Mathews 1979). Also, as noted above, the column density of the extended transition region is apparently variable from object to object. Thus, since the strengths of the Fe II optical lines in the Kwan and Krolik model depend sensitively on the column density while the strengths of the very optically thick Fe II UV lines do not, it is probable that the predicted relative strengths of the optical or UV lines among themselves should be more reliable than comparisons between the UV and optical lines. The same point presumably holds true for the Phillips model; a change in $\tau_{\lambda 2344}$ would significantly alter the UV-to-optical ratios but not the relative UV ratios. Note that the Kwan and Krolik model, which has a larger value of $\tau_{\lambda 2344}$ than the Phillips model, has a significantly larger value of Fe II λ4570/Fe II λ2500. For observational confirmation of this point, compare the spectra of 4C 31.63 and 4C 16.30 in Figure 1.

In general, the observational data listed in Table 2 agree tolerably well (roughly within a factor of 2 for the relative Fe II strengths) with the predictions described above given the inherent uncertainties: inaccuracies in calculating the relative abundance and ionization of Fe and Mg, poorly known atomic data (particularly the collision strengths), and the sensitivity of the models to $T_e$ and the column density. However, a better idea of the accuracy of the entire line lists of the Kwan and Krolik and the Phillips models in predicting the blends as they are actually seen in observed spectra can be obtained via the construction of synthetic spectra in order that complications such as the other emission lines, the λ3000 bump, and possible λ2200 dust absorption may be properly considered. In the comparison between the observed spectra and the synthetic spectra, I will concentrate on the relative strengths of the Fe II UV multiplets and largely ignore the relative strengths of the UV blends to the optical Fe II blends (which depend on the column density) and the absolute strengths of the UV Fe II blends relative to Mg II (which depends on the ionization and abundance of Mg and Fe).

Synthetic spectra (which are described in much more detail in Grandi 1982) were constructed as follows: Hydrogen lines were included with the "mean quasar" line ratios Lyα/Hα/Hβ/Hγ = 2.0/1.0/0.33/0.14 (Puetter *et al.* 1981) with subsequent Balmer line strengths (up to H29) according to the case B, $T_e = 10^4$ K, $N_e = 10^6$ cm$^{-3}$ calculations of Brocklehurst (1971) and Paschen lines at 0.32 the strength of their colevel Balmer lines. Mg II λ2798 and C III] λ1909 were included (with relative intensities to Hα of 0.25) as were several weak He I and He II lines. A power law, of spectral index $\alpha = 0.8$, was included in the synthetic spectra such that the equivalent width of Hβ is 100 Å. Two photon emission was included with an integrated strength compared to Hα of 0.1. The strengths of the optically thin Balmer and Paschen continua were parametrized such that $F^{BC}$/Mg II λ2798 = 5 and $F^{PC}$/Mg II λ2798 = 3.25 where $F^{BC}$ is the integrated strength of the Balmer continuum (at the model value of $T_e = 12{,}500$ K). To facilitate comparisons with the values listed in Table 1, $F^{BC}$/Mg II λ2798 = 5 at $T_e = 12{,}500$ K corresponds to $F^{BC}$/Mg II λ2798 = 4 at $T_e = 10{,}000$ K.

Finally, the synthetic spectra were velocity broadened by convolution with a "Lorentzian" shaped function with FWHM = 4500 km s$^{-1}$. A small amount of reddening due to dust exterior, but close to, the emission line region is assumed to modify the emitted spectrum. The reddening curve derived by Seaton (1979) for galactic dust has been used assuming $E(B-V) = 0.02$. A plot of a synthetic spectrum as described, but with no Fe II emission, is shown in Figure 2*a*. Aside from the lack of narrow [O III] forbidden lines, and ignoring the bumps and wiggles ascribed to Fe II, Figure 2*a* is a reasonable match for the sample quasar spectra shown in Figure 1.

Figures 2*b* and 2*c* show synthetic spectra with the addition of Fe II emission predicted by the models of Phillips and of Kwan and Krolik, respectively. The Fe II emission in each case is scaled such that Fe II UV2/Mg II λ2798 = 0.3 (in the complete calculation of Kwan and Krolik, Fe II UV2/Mg II λ2798 = 0.08). This corresponds to Fe II λ2500/Mg II λ2798 = 0.78 for the Phillips model and 1.2 for the Kwan and Krolik model; the observed value is 0.98. The relative strengths of the components of each multiplet in the Phillips model were also used in the construction of synthetic spectra with the Kwan and Krolik model, scaled to the appropriate total multiplet strength. This is a reasonable assumption since, at least for the UV multiplets, the components of each multiplet are all optically thick.

Intercomparison of Figures 1, 2*a*, and 2*b* reveals clearly the triumphs and failures of the attempts to model the UV blends of Fe II. Some of the features of the observed composite scans are well reproduced in both synthetic spectra: the bump on the blue side of Mg II λ2798 (due to UV62 and UV63) and the apparent lack of emission near λ2650 (the "trough" discussed by Jauncy *et al.* 1978). On the other hand, the three prominent UV blends λ3200, λ2950, and λ2500 look quite different in the observed data than in either synthetic spectrum. In place of the observed broad hump of emission between λλ2250 and 2650 that I call the λ2500 blend, the synthetic spectra show four distinct peaks corresponding to UV4 at λ2261, UV2 at λ2385 (with weaker contributions from UV3 and UV35 at λλ2351, 2369 on the blue wing), UV34 and UV33 at λ2465, 2518, and UV1 at λ2615. The relative strengths of these four distinct features varies between the two models, but

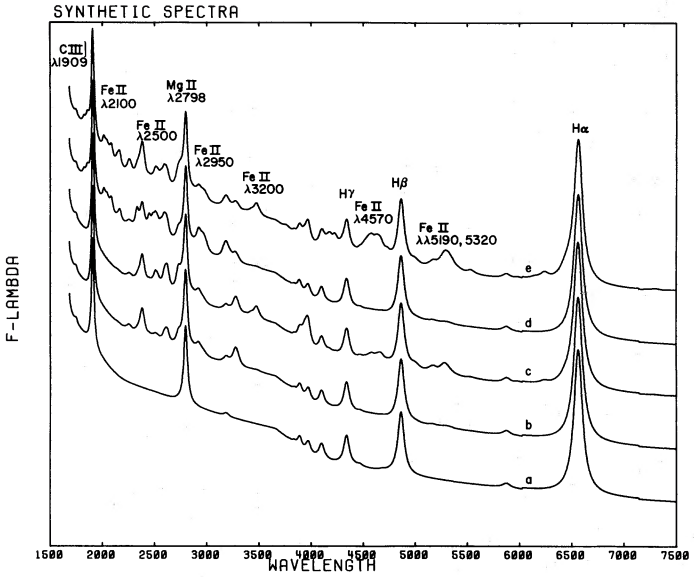


FIG. 2.—Synthetic spectra of quasars are plotted on a relative $F_\lambda$ vs. rest wavelength scale. Line 2*a* shows a synthetic spectrum without Fe II emission; line 2*b* shows a synthetic spectrum with the Phillips Fe II model; line 2*c* shows a synthetic spectrum with the Kwan and Krolik Fe II model: line 2*d* shows a synthetic spectrum with the ad hoc Fe II model described in the text; and line 2*e* shows a modified Kwan and Krolik Fe II model, also described in the text. All five spectra are plotted at the same scale with equal vertical offsets applied (the horizontal axis corresponds to zero flux for line 2*a*).

neither has emission to fill the obvious gaps near λ2325, λ2440, and λ2550. The predicted λ2950 blend seems to peak too sharply and too far to the blue as compared to the observed blend. The predicted λ3200 blend is totally different from the observed blend. Multiplets 6 (λ3199) and 7 (λ3180) are quite weak in the predicted spectra, while multiplet 1 (λ3281) seems too strong. Also, as noted above, since both models lack the 8 eV terms, the λ2100 blend is totally absent in the synthetic spectra.

Thus, there seem to be significant differences between the predicted synthetic spectra based on two extensive Fe II calculations and the observed spectra, despite the apparent agreement between the predicted and observed blend strengths noted in Tables 2 and 3. Several caveats to the models are obvious: poorly known *A*-values and collision strengths. Also, despite attempts to isolate any effects of the Fe II column density by considering only relative strengths among the UV lines, these UV lines still cover a wide range in transition probability which will make optical depth effects nonnegligible. Of course, if some of the blends under discussion are not due to Fe II, then a disagreement between the models and the observations would not be unexpected. However, with the notable exception of C II] λ2326, there are no likely candidates for alternative identifications.

A useful exercise to understand the failure of the two model generated synthetic spectra to predict accurately the observed spectra is to try to modify the predictions of the models to force better agreement with the observations. Hopefully, this will lead to an indication of the proper direction for the next round of models. Also, as pointed out by Wills, Netzer, and Wills (1980), an accurate description of the observed Fe II spectra in quasars must include lines from the 8 eV terms of Fe II that are not included in the Phillips or Kwan and Krolik models. As a first, quite unphysical, step, I will abandon caution and arbitrarily modify individual UV Fe II multiplet strengths ignoring altogether other multiplets from the same upper level. Such an ad hoc synthetic spectrum might be useful for no better reason than as a reasonable representation of the observed Fe II spectrum which can be utilized for other studies (see Grandi 1982, for example).

The following recipe for the ad hoc Fe II spectrum holds promise. Starting from the Phillips model, decrease the strength of multiplet 1 by a factor of 2 and increase the strength of multiplets 6 and 7 by a factor of 5 each to rectify the shape of the λ3200 blend. For the λ2950 blend, the strength of UV 60 should be increased by a factor of 2 and the strength of multiplet 8 increased by a factor of 10. Major surgery is indicated for the λ2500 blend; perhaps multiplets UV 34, UV 33, and UV 64 could be increased by factors of 8, 4, and 15, respectively. Unfortunately, there are *no* multiplets in the 16 term model Fe II atom which could fill the obvious gaps at λ2325 and λ2440. Some of these suggested increases might plausibly be accounted for by an increase in the electron temperature which would more heavily populate the upper three terms of the 16 term atom ($z^4F^\circ$, $z^4D^\circ$, and $z^4P^\circ$) and justify stronger emis-

sion in multiplets 6, 7, and 8. However, the machinations involving the λ2500 blend lack even this justification.

As a first attempt in extending the Fe II model atom, Wills, Netzer, and Wills crudely calculate the expected strengths (including a very uncertain correction for optical depth effects) of 28 multiplets (out of the hundreds possible) from 15 higher terms of Fe II in comparison to the strength of UV 35. I have included all of these multiplets longward of λ1800 in the ad hoc synthetic spectrum to try to predict the λ2100 blend and to see if the gaps in the λ2500 blend can be filled. However, the strengths calculated by Wills, Netzer, and Wills seem to be much too weak to generate the observed λ2100 feature (again, perhaps indicating an underestimate of the electron temperature?). Hence, I have arbitrarily upped their strength relative to UV 35 by a factor of 25.

The resulting ad hoc synthetic spectrum is shown in Figure 2*d* and the individual multiplet strengths are listed in Table 4 (strengths that were modified are italicized). Not surprisingly, the match with the observed quasar spectra shown in Figure 1 is reasonably good. The predicted λ2950 and λ3200 blends appear realistic as does the newly generated λ2100 blend. The troublesome λ2500 blend still looks somewhat choppier than is observed, but, except for the pronounced gap near λ2440, it would be an acceptable match with the observations. Clearly, this game of arbitrarily adjusting multiplet strengths is ultimately futile, but it does indicate the direction for further models.

Following the idea that the upper Fe II levels should be relatively more populated than in the existing models, a modified Kwan and Krolik model can be constructed that crudely corresponds to a higher electron temperature. How this higher temperature might be reconciled with the low (~8000 K) values found in the Fe II zone in the complete emission cloud model of Kwan and Krolik (1981) is not obvious, however. In any case, the modified Fe II spectrum was constructed by requiring that (in order of decreasing energy) all lines from the $z^4P^\circ$ upper term in the Kwan and Krolik model be increased in strength by a factor of 7, all lines from the $z^4D^\circ$ upper term be increased by a factor of 4, all lines from the $z^4F^\circ$ term be increased by a factor of 3, all lines from the $z^6P^\circ$ and $z^6F^\circ$ upper terms remain the same, and all lines from the $z^6D^\circ$ upper term be decreased by a factor of 2. The lines from the 8 eV levels as listed in Table 4 are also included.

The resulting synthetic spectrum is shown in Figure 2*e*. The λ2100, λ2950, and λ3250 blends appear to be reasonable matches to the observed spectrum, while the blends near λ4000 do not (as is the case for the unmodified Kwan and Krolik model as well). Nonetheless, the modified Kwan-Krolik synthetic spectrum would be a promising representation of actual quasars except for the λ2500 blend. Thus, if some other means of explaining the observed λ2500 blend can be found, higher temperature models seem to be hopeful possibilities for the future.

The λ2500 blend seems to present a greater challenge. Yet, only a cursory glance at the multiplet table reveals dozens of Fe II lines leaving the 8 eV terms that could contribute to this troublesome blend that were not included in the initial model of Wills, Netzer, and Wills (1980). For example, multiplet UV 148 (λ2450) has a large transition probability and thus will probably be strong and could very well help fill the λ2440 gap in the λ2500 blend. Only rather detailed models, including radiative transfer effects, can properly assess the strengths of these lines.

Thus, future models of optically thick, collisionally excited Fe II must include many more terms (including the odd parity terms near 8 eV and the low lying doublet terms which can feed some of these 8 eV levels) than the 16 considered previously. As mentioned above, models should also be calculated with higher values of the electron temperature than 10,000 K. As a first attempt, a calculation, such as Phillips's 16 term model, divorced from a complete quasar emission line cloud model and using a simple radiative transfer scheme would be quite useful.

To summarize this section: the collected observations of Fe II emission blends are compared to various theoretical calculations of collisionally excited, optically thick Fe II emission. Attention is restricted to relative strengths among the Fe II UV multiplets to prevent undue sensitivity to the Fe II column density. Despite reasonable agreement between observed and predicted blend strengths, synthetic spectra constructed from two extensive Fe II calculations fail to reproduce the observed spectra. From an ad hoc effort to reproduce the observations by arbitrarily changing the Fe II multiplet strengths, it is deduced that future correct models for the Fe II emission in quasars must include many more atomic terms than the current 16 term calculations and that higher values of the electron temperature than 10,000 K should be considered.

I wish to thank J. L. Weiland for performing most of the measurements listed in Table 1; M. M. Phillips for the detailed output from his model and for conversations; J. H. Krolik and R. C. Puetter for preprints and conversations; and M. M. Phillips, J. M. Shuder, J. A. Baldwin, E. J. Wampler, and D. E. Osterbrock for donations to the data bank.

REFERENCES

Baldwin, J. A. 1975*a*, *Ap. J.* (*Letters*), **196**, L91.
_____. 1975*b*, *Ap. J.*, **201**, 26.
_____. 1977, *M.N.R.A.S.*, **178**, 67P.
Blumenthal, G. R., and Mathews, W. G. 1979, *Ap. J.*, **233**, 479.
Boksenberg, A., and Netzer, H. 1977, *Ap. J.*, **212**, 37.
Brocklehurst, M. 1971, *M.N.R.A.S.*, **153**, 471.

Canfield, R. C., and Puetter, R. C. 1981, *Ap. J.*, **243**, 381.
Collin-Souffrin, S., Joly, M., Heidmann, N., and Dumont, S. 1979, *Astr. Ap.*, **72**, 293.
Collin-Souffrin, S., Dumont, S., Heidmann, N., and Joly, M. 1980, *Astr. Ap.*, **83**, 190.
French, H. B., and Miller, J. S. 1980, *Pub. A.S.P.*, **92**, 753.
Grandi, S. A. 1982, *Ap. J.*, submitted.
Grandi, S. A., and Phillips, M. M. 1979, *Ap. J.*, **232**, 659.
_____. 1980, *Ap. J.*, **239**, 475.
Jauncy, D. L., Wright, A. E., Peterson, B. A., and Condon, J. L. 1978, *Ap. J.* (*Letters*), **219**, L1.
Kwan, J., and Krolik, J. H. 1979, *Ap. J.* (*Letters*), **233**, L91.
_____. 1981, *Ap. J.*, **250**, 478.
Miller, J. S., Robinson, L. B., and Schmidt, G. D. 1980, *Pub. A.S.P.*, **92**, 702.
Netzer, H. 1980, *Ap. J.*, **236**, 406.
Neugebauer, G., Oke, J. B., Becklin, E. E. and Matthews, K. 1979, *Ap. J.*, **230**, 79.
Osterbrock, D. E. 1977, *Ap. J.*, **215**, 733.
Phillips, M. M. 1977, *Ap. J.*, **215**, 746.
_____. 1978*a*, *Ap. J.* (*Suppl.*), **38**, 187.
_____. 1978*b*, *Ap. J.*, **226**, 736.
_____. 1979, *Ap. J.* (*Suppl.*), **39**, 377.
Puetter, R. C., Smith, H. E., Willner, S. P., and Pipher, J. L. 1981, *Ap. J.*, **243**, 345.
Richstone, D. O., and Schmidt, M. 1980, *Ap. J.*, **235**, 361.
Robinson, L. B., and Wampler, E. J. 1972, *Pub. A.S.P.*, **84**, 161.
Seaton, M. J. 1979, *M.N.R.A.S.*, **187**, 73P.
Soifer, B. T., Neugebauer, G., Oke, J. B., and Mathews, K. 1981, *Ap. J.*, **243**, 369.
van Regemorter, H. 1962, *Ap. J.*, **136**, 906.
Wampler, E. J., and Oke, J. B. 1967, *Ap. J.*, **148**, 695.
Wills, B. J., Netzer, H., and Wills, D. 1980, *Ap. J.* (*Letters*), **242**, L1.
Wills, B. J., Netzer, H., Uomoto, A. K., and Wills, D. 1980, *Ap. J.*, **237**, 319.

STEVEN A. GRANDI: Department of Astronomy, University of California, Los Angeles, 405 Hilgard Ave., Los Angeles, Ca 90024